Dear Stef Lhermitte and anonymous referees,

Thank you very much again for your thorough and very constructive review of our manuscript. We tried to address all the issues and questions that came up during the review process and revised the manuscript accordingly. We are confident that your comments improved the manuscript's quality a lot. Thank you for this productive review process.

First, we would like to apologize for the brevity of some of our comments in the interactive discussion. It is the first time that we undergo this form of review process and we expected the review to be similar to a chat.

As advised, we revised our manuscript based on the comments related i) to similar observation/models for melt ponds on grounded ice and ii) to the novelty.
In our revised version, we restructured the Introduction and now refer to the work of Legleiter et al. (2014) and Tedesco and Steiner (2011) on supraglacial lakes on the Greenland ice sheet. We describe their work and reason why both models are unsuitable for melt ponds on sea ice. We also describe that the great challenge in both studies is the wide range of depth in supraglacial ponds. As suggested by Referee #2 we further specified the description of the models of Lu et al. (2016) and Malinka et al. (2018) and formulated an educated guess about the reasons for their problems in pond depth retrieval. Please read our restructured Introduction for further details.
Thanks to your constructive review and editorial, we highlighted the important findings that underline the novelty of our model (see Abstract and Conclusion). (i) Our model uses near infrared light for the retrieval of melt pond bathymetry on Arctic sea ice with unprecedented accuracy and without having to consider bottom albedo. (ii) It addresses the influence of changing sun zenith angle and (iii) is of semi-empirical nature due to the model training on simulated data. This has the advantage that our model - in contrast to purely empirical models such as the one described in Legleiter et al. (2014) - is unbiased towards a certain range of depth or bottom albedo.
Although the model is fitted for ponds on sea ice, it would be worth testing it on shallow pond measurements from supraglacial lakes. We added this idea to the discussion section. However, we believe that this analysis needs to be done in a separate study.

We further added information about the difference between Rrs and R to the discussion section. As Stef correctly pointed out albedo may be used as a proxy for satellite measurements when assuming lambertian behavior. However, this assumption is not complied over water surfaces, which do not reflect lambertian but are characterized by Fresnel reflection. A direct comparison between Rrs and R measurements over water is therefore not trivial. In addition, satellite and airborne remote sensors acquire radiance and not irradiance. For this reason, Rrs has replaced albedo in remote sensing and we chose it for our measurements accordingly.

In the following tables, we reply to the referee comments in more detail.

We are confident that our revised version fulfils the requirements for publication in The Cryosphere.

Best regards,

Marcel König and Natascha Oppelt

Referee #1

Major comments

Comment	Answer
The authors make the assumption that the reflectance spectra of light and dark bare	We chose the bare ice surfaces because we did not observe a surface scattering layer (compare

ice can serve as proxies for the reflectance spectra of the pond floors of light and dark ponds. I think this likely not true. Melting bare ice typically develops a surface scattering layer, which is likely not present where the ice is ponded. If I follow the arguments made by the authors later in the manuscript, it may turn out that their model is very insensitive to this assumption, which is good. But, I do think the assumption merits some discussion when it is first presented (Section 2.1.1).	Figure 1A,B) and made the assumption the corresponding spectra serve as good candidates for pond bottom spectra. We added this information as well as our assumption to Section 2.1.1.
It appears that there are 49 data points used in the validation of this model. That sounds like a large number, but I am concerned that they all come from only 3 distinct ponds. It is not stated whether the site was first-year or multiyear ice. Presumably, unless the pond floors were rafted ice, the optical properties of the pond floors for each pond were likely homogeneous? I suspect there is considerable variability in pond floor properties beyond what was sampled in these three ponds.	As we mentioned in our first reply, no ice cores were analyzed to define the ice types below the ponds. Ice thickness measurements from June 31 however indicate that the bright ice is older (possibly second year or multiyear ice) than the dark one (possibly a refrozen lead). We added these details to Section 2.1.2. Regarding the bottom texture of the ponds, we likewise added a description and field photographs to Section 2.1.2. We also added a paragraph to the discussion in Section 4.2 pointing towards the limited amount of variability within in three ponds and highlighted the need for more data.
I wonder if it would be useful to compare the spectra shown in Fig. 5 with the spectra shown in Fig. 5 of Light et al. (2015; https://doi.org/10.1002/2015JC011163)? Eyeball comparison suggests the albedos in that study are spectrally flatter than the reflectance spectra shown here.	Of course, we were aware of the large database of albedo spectra from previous studies. Yet, as we pointed out above, a comparison of albedo and Rrs measurements is not trivial due to the non-lambertian characteristics of the water surface. We refer to this issue in Section 4.1.1.
In the discussion (line 206) the authors declare the “universality” of this approach. I would argue that data from 3 melt ponds (all observed on the same day) likely does not show convincing universality! Also, the fact that the model is only valid for solar angles between 58.9 and 61 degrees makes it not truly universal.	We agree that “universal” was overstated and therefore used the term “applicability” instead. You are right that the limited amount of spectra as well as the variability of depth and bottom characteristics in the test data requires more field data for validation. We restructured the discussion accordingly (Section 4.2). We also agree that more testing on different sun zenith angles is desirable. The model, however, is valid for all sun zenith angles. In comparison to purely empirical models trained on field measurements only, our novel methodology based on a simulated spectral library has the virtue that variations due to sun zenith angle are accounted for by the model (compare Section 2.2.3).

Minor comments

We addressed most of the minor comments according to your suggestions and as described in the first response. Only regarding your last comment, we came up with a new formulation.

line 245: "widely independent"? This needs to be clarified. Is "independent" sufficient?	We agree that the formulation was not precise and changed the sentence to: "We successfully developed a model to accurately derive the depth of melt ponds on Arctic sea ice without having to consider the bottom ice characteristics of the pond."

Referee #2

Major comments

The authors provide no justification for deriving melt pond depths in the introduction. Do deeper ponds have a substantial impact on sea ice energy balance? Are melt pond volumes required inputs for sea ice modeling? From the introduction, it appears we only need melt pond fraction for forecasting September sea ice area. Without these statements, it is difficult to understand why the authors have put effort into deriving a model for simulating melt pond depths.	You are right that the justification was too sparse in the previous version of the manuscript. We therefore included some references in the revised introduction.
The conclusions of this study are not supported by the evidence. In L204-205, the authors claim that their approach is "universal" and able to derive depths from dark and bright melt ponds. However, in the results, it looks like the R2 for the dark ponds is much worse than for bright ponds. It is misleading to claim that their model is accurate for dark ponds.	As we pointed out in our first reply and in the reply to Referee #1, we agree that "universal" is not the correct term and replaced it with "applicability". As proposed in our previous reply we expanded the discussion according to your comment (Section 4.2). We point out that R2 is much worse for the dark pond but discuss that this is due to the small number of samples and the shallowness of the measurements. The similar RMSE in dark and bright ponds proves that the model's accuracy is similar in both cases, which is also illustrated in Figure 11B.
Likewise, the authors state that their study provides "the most comprehensive set of Rrs and depth measurements from Arctic melt ponds...". However, the study only presents 49 depths from three melt ponds with a depth range of 6 to 25 cm. A quick search of the literature reveals that this statement misleading. Malinka et al.(2018) https://doi.org/10.5194/tc-12-1921-2018 used coincident depth and spectra measurements from three different areas of the Arctic (SHEBA experiment in 1998, Barrow in2008 and the Polarstern in 2012). Tedesco and Steiner (2011)	Thanks to your valuable comment, we revisited the studies you mentioned and restructured the introduction and discussion sections, which improved the quality of the manuscript a lot. We integrated the work of Legleiter et al. (2014) and Tedesco and Steiner (2011) into the introduction emphasizing the difference between ponds on sea ice and glaciers and the consequences for model development. In the discussion section, we refer to the albedo data sets from melt ponds on sea ice and explain that a comparison of R and Rrs is not trivial due to the non-lambertian behaviour of the water

doi:10.5194/tc-5-445-2011 and Legleiter et al.(2014) doi:10.5194/tc-8-215-2014 collected hundreds if not thousands of coincident depth and spectra measurements in a melt pond on the Greenland Ice Sheet that had depths of up to 10 m. The authors should review this literature (including those studies from the Greenland Ice Sheet) before making such claims.	surface. We deleted the paragraph you were referring to because it only caused confusion without really contributing to the manuscript. Instead, we placed the statement in the discussion section where we use it to provide reason for more measurements in order to overcome the limited variability in our test data.
The problems outlined above raise questions about the novelty and significance of the study. The only real result in the abstract is that the "...results indicate that pond depth is retrievable from optical data under clear sky conditions". As far as I understand (and based on the references in the previous paragraph) this is not a novel finding. The authors should think more deeply about how their study advances our understanding and build on previous research. However, in the present version, this study may only have limited interest to the cryospheric community	Thanks to your thorough review of our manuscript and the reference to other studies, we were able to restructure and improve our manuscript. In the updated abstract and conclusion we explicitly point out the novelty of our approach which we also describe at the beginning of this letter. The three novelties are: (i) The utilization of near-infrared light for pond depth retrieval with unprecedented accuracy. (ii) The adjustment to changing sun zenith angle. (iii) The semi-empirical nature of the model, i.e. training on simulated data and testing on field data. We further hypothesize that the model may improve the bathymetry mapping in shallow water areas of supraglacial lakes.
The writing style is vague in many places. For example: L5: "Key elements" L33:"easy-to-use" L96: "expert knowledge" L234: "hitting the same spot" L235: "tricky" L245:"widely independent" The authors should consider being more specific where possible to improve the readability	We tried to be more specific and rewrote the examples you mentioned where possible. Likewise, we tried to be as specific as possible in the new paragraphs of the updated manuscript.

Specific comments

We addressed most of the comments as proposed in our first reply.

L28-209: Considering the apparent similarity between this work and Malinka et al. (2018), the authors should consider adding a much more thorough description of how the two models differ in the introduction.	In the updated introduction, we expanded the description of the model described in Malinka et al. (2018) and point out the major differences.
P126: Please justify why pond depth is extrapolated to 1 m when the maximum pond depths in this study were 25 cm.	The intention of our study was the development of a model that allows pond depth retrieval from remote sensing data. Therefore, it needs to be applicable to ponds in all states of the melting process. Ponds on sea ice are usually shallower than 100 cm because pond depth is restricted by ice thickness.

	It was not our aim to find the optimal model for our field data set. Instead, we wanted to develop general approach that is transferrable. We therefore generated a spectral library for model training and used the field data for testing.

A linear model to derive melt pond depth on Arctic sea ice from hyperspectral data

Marcel König[1], Natascha Oppelt[1]

[1]Department of Geography, Kiel University, Kiel, 24118, Germany

Correspondence to: Marcel König (koenig@geographie.uni-kiel.de)

Abstract. Melt ponds are key elements in the energy balance of Arctic sea ice. Observing their temporal evolution is crucial for understanding melt processes and predicting sea ice evolution. Remote sensing is the only technique that enables large-scale observations of Arctic sea ice. However, monitoring ~~vertical~~ melt pond ~~evolution~~ deepening in this way is challenging because most of the optical signal reflected by a pond is defined by the scattering characteristics of the underlying ice. Without knowing the influence of melt water on the reflected signal, the water depth cannot be determined. To solve the problem, we simulated the way melt water changes the reflected spectra of bare ice. We developed a model based on the slope of the log-scaled remote sensing reflectance at 710 nm as a function of depth that is widely independent from the bottom albedo and accounts for the influence of varying sun zenith angles. We validated the model using 49 in situ melt pond spectra and corresponding depths from ponds on dark and bright ice. Retrieved pond depths are ~~precise~~ accurate ($RMSE$ = 2.81 cm) and highly correlated with in situ measurements (r = 0.89; p = 4.34e-17). The model further explains a large portion of the variation in pond depth (R^2 = 0.74). Our results indicate that our model enables the accurate retrieval of pond depth on Arctic sea ice ~~is retrievable~~ from optical data under clear sky conditions without having to consider pond bottom albedo. This technique is potentially transferrable to hyperspectral remote sensors on UAVs, aircraft and satellites.

1 Introduction

Melt ponds on sea ice are key elements for the Arctic energy budget. They are a main driver of the ice-albedo-feedback mechanism (Curry et al., 1995) and affect the mass and heat balance of sea ice (e.g. Flocco et al., 2012; Perovich et al., 2009). Observations of ~~P~~pond evolution can be linked to observations of sea ice, ocean and atmosphere (e.g. Inoue et al., 2008; Polashenski et al., 2012; Webster et al., 2015), for validation of ice and climate models (e.g. Flocco et al., 2012) and future sea ice prediction (e.g. Schröder et al., 2014). ~~, e.g. Schröder et al. (2014) show that spring melt pond fraction can be used to forecast September sea ice area.~~In the context of climate change it is therefore important to increase our understanding of how melt ponds on sea ice change (Lee et al., 2012).

Recent efforts were made to observe the evolution of melt pond fraction with satellite data (e.g. Istomina et al., 2015a, 2015b; Rösel et al., 2012; Tschudi et al., 2008; Zege et al., 2015) but little focus has been put on melt pond depth despite its relevance for many applications. Melt pond depth is a parameter in the Los Alamos sea ice model CICE (Flocco et al., 2012; Hunke et al., 2013) and the ECHAM5 general circulation model (Pedersen et al., 2009). Lecomte et al. (2011) used pond depth to parameterize melt pond albedo in a snow scheme for the thermodynamic component of the Louvain-la-Neuve sea ice model. Holland et al. (2012) related pond water volume to surface meltwater fluxes in the Community Climate System Model, version 4; and Palmer et al. (2014) used melt pond depths to model primary production below sea ice. Liu et al. (2015) reckon that climate models and forecast systems that account for realistic melt pond evolution "seem to be a worthy area of expanded research and development" (Liu et al., 2015) and question the suitability of statistical forecasting methods in the context of the changing Arctic pointing towards the need for regular observations with large spatial coverage.

Synoptic observations of melt pond evolution are only possible with satellite remote sensing. Optical sensors with an adequate spatial resolution that operate in the visible (VIS) and near infrared (NIR) wavelength regions enable a monitoring of pond water characteristics. The reflected optical signal from melt ponds without ice cover contains information on the pond water, the pond bottom, i.e. underlying ice~~,~~ and skylight reflected at the water surface.
~~The reflected optical signal from open melt ponds contains information on the pond water, the pond bottom, i.e. underlying ice, and skylight reflected at the water surface. The color of melt ponds ranges from bright blue to almost black and is primarily defined by the scattering and to a lesser degree by the absorption characteristics of the pond bottom (Lu et al., 2016, 2017).~~
Some studies investigated the potential to map the bathymetry of melt ponds with optical data in supraglacial lakes on the Greenland ice sheet. Tedesco and Steinar (2011) used the model of Philpot (1989) for optically shallow water and resampled hyperspectral reflectance measurements from below the water surface to Landsat and MODIS bands in order to explore its capability to derive the depth of a supraglacial lake. Due to the strong absorption of water in the near infrared, they limited the data range to 450 – 650 nm and excluded depth measurements < 1 m "because of the relatively small sensitivity of the reflectance data in the Landsat and MODIS blue and green bands to shallow waters" (Tedesco and Steiner, 2011). In comparison with shallow water sonar measurements, they ~~report~~ underestimated~~ion of~~ depth by -23.7% and -42.7% for Landsat bands 1 and 2, respectively. Legleiter et al. (2014) used hyperspectral remote sensing reflectance measurements ~~from~~ above the water surface to map the bathymetry of supraglacial lakes and streams. They used an optimal band ratio analysis to find suitable band combinations for calibrating an empirical model based on field measurements ~~from two streams and one lake~~ on the Greenland ice sheet. A model based on two bands in the yellow-orange wavelength region resulted in a~~n~~ R^2 of 0.92 and a standard error of 0.47 m for depths ranging between 0.31 m and 10.45 m. While this accuracy may be sufficient for glacial ~~ponds~~lakes, the maximum depth of ponds on sea ice is restricted by its thickness and therefore seldom exceeds 1 m (e.g. Morassutti and Ledrew, 1996; Perovich et al., 2009).

The color of melt ponds on sea ice ranges from bright blue to almost black and is primarily defined by the scattering and, to a lesser degree, by the absorption characteristics of the pond bottom (Lu et al., 2016, 2017). Different radiative transfer models for melt ponds on sea ice exist ~~(e.g. Lu et al., 2017; Malinka et al., 2018)~~ but their capability to derive pond depth varies. Lu et al. (2016, 2017) developed a two-stream radiative transfer model to retrieve pond depth and the thickness of the underlying ice from RGB images but did not find a clear relationship between simulated and measured pond depth using the data by Istomina et al. (2016). To our knowledge, the most accurate model is the one presented in Malinka et al. (2018) resulting in a~~n~~ R^2 of 0.62 ($N = 26$) ~~against~~for in situ ~~for~~ pond depths between 6 cm and 50 cm acquired under and different illumination conditions. Their analytical two-stream radiative transfer model links ~~pond~~ the spectral albedo of ponds between 350 and 1300 nm at various sky conditions to pond depth and transport scattering coefficient and thickness of the bottom ice. Fitting these parameters during ~~I~~inverse computation~~s~~ of in situ datasets from three field campaigns accurately reproduced in situ albedo spectra (relative root mean square difference ($rRMSD$) < 1.5%) but pond depth retrieval was more uncertain ($rRMSD = 65\%$).

~~Therefore, our motivation is to 1) improve the limited accuracy of existing models and 2) develop an easy-to-use approach for deriving melt pond depth using hyperspectral data.~~

We hypothesize that instead of using the entire spectrum, selecting bands ~~at certain wavelengths~~in the near infrared wavelength region improves the retrieval of pond depth on sea ice from optical data. The penetration depth of light into water is highest in the blue region of the electromagnetic spectrum and decreases with increasing wavelength, i.e.~~. This means that~~ with increasing wavelength the influence of the water column's attenuation on the optical signal increases (Pope and Fry, 1997). Mapping the bathymetry of supraglacial lakes with a two-band model is challenging, because the attenuation of water is wavelength dependent and the range of depth is wide. For shallow ponds on sea ice Morassutti and Ledrew (1996) stated that the influence of water absorption on the pond albedo increases towards the ~~infrared~~ NIR wavelength region, ~~and~~ Lu et al. (2016) found that pond albedo significantly depends on pond depth in the wavelength region between 600 nm and 900 nm. In this paper, we therefore present a ~~simple~~ linear pond depth model for Arctic sea ice, based on the absorption of near infrared light in water ~~to retrieve pond depth~~ ~~on Arctic sea ice~~ from hyperspectral optical measurements under clear sky conditions.

2 Methods

We use spectral data of bare ice surfaces to simulate melt pond spectra for model development, and validate the model with in situ melt pond measurements acquired during RV *Polarstern* cruise PS106 in summer 2017.

2.1 Observational data

We used two instrument setups for acquisition of optical data. For most measurements, we used a combination of two Ocean Optics STS-VIS spectrometers (Ocean Optics Inc., USA). One spectrometer pointing downwards and equipped with a 1° fore optic; the other pointing upwards and equipped with a cosine collector. Both instruments cover the wavelength region from ~ 340 nm to ~ 820 nm with a spectral sampling interval~~rate~~ < 1 nm and an spectral resolution of 3.0 nm (Ocean Optics, 2019). We used a Labsphere Spectralon 99 % diffuse reflectance standard (Labsphere Inc., USA) as white reference and applied the data from the second spectrometer to correct the reflectance spectra for changes in downwelling irradiance. For each measurement, we computed the average of 30 single spectra. Both instruments were mounted to the end of a 1 m long pole to avoid influences of the polar clothes on the measurements. We also attached a camera to the setup to take photographs of each measurement site (Figure 1).

Some of the data used in this study ~~was~~ were acquired within the scope of an angle-resolving BRDF ~~goniometer~~ experiment. For these measurements, we used an Ibsen Freedom VIS FSV-305 spectrometer (Ibsen Photonics A/S, Denmark) with a spectral sampling rate < 1 nm and a spectral resolution of 1.8 nm covering the wavelength range from ~ 360 nm to ~ 830 nm (Ibsen Photonics, 2019). The spectrometer ~~has been~~was equipped with an optical fiber and a 1° fore optic that were attached to a field goniometer (Figure 2). We used the above-mentioned Spectralon panel as white reference after each azimuthal scan and computed an average reflectance from 20 spectra.

The quantity measured with both spectrometer setups is the remote sensing reflectance $[sr^{-1}]$ (R_{rs}) above the water surface:

$$R_{rs} = \frac{L_u}{E_d}, \tag{1}$$

where L_u is upwelling radiance $[W/(m^2\ nm\ sr)]$ measured by the downwards-pointing sensor and E_d is downwelling irradiance $[W/(m^2\ nm)]$ derived from the Spectralon measurement as

$$E_d = \frac{L_S \cdot \pi}{R_S}, \tag{2}$$

where R_S is the isotropic reflectance of the Spectralon panel, and L_S is a radiance measurement $[W/(m^2\ nm\ sr)]$ of the Spectralon panel.

2.1.1 Ice spectra

On 15 June 2017, we used the Ocean Optics setup to collect~~ed~~ spectra from three bright and one dark bare ice surface ~~with the Ocean Optics~~ (Gege et al., 2019) that were missing the typical surface scattering layer (Figure 1A, B). We therefore assume that their optical properties are comparable to pond bottoms. ~~setup~~ Illumination was ~~under stable~~ diffuse ~~illumination conditions~~ and stable indicated by the negligible standard deviation of the 30 spectra contained in one measurement (Figure 1C).

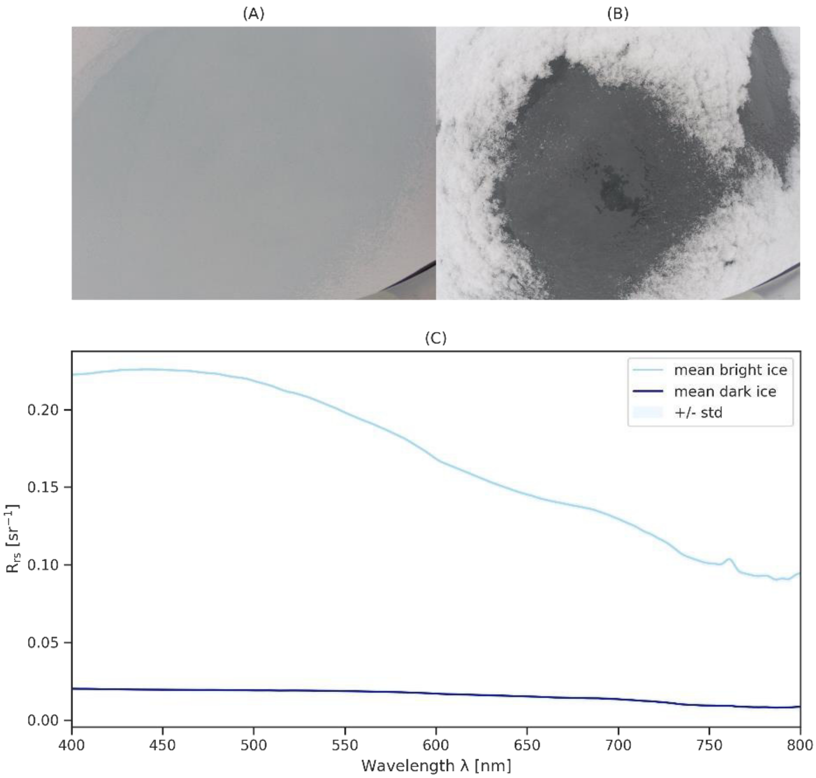

Figure 1: Photos of bright (A) and dark (B) bare ice surfaces and respective reflectance spectra (C). We took the photos from approximately 50 cm (A) and 30 cm (B) above the surface.

On 2 July 2017 between 22:28 UTC and 23:11 UTC, we performed twelve nadir measurements of a bare ice surface, likewise missing a surface scattering layer (Figure 2A), under clear sky conditions and a mean sun zenith angle of 74.89° with the Ibsen setup (Gege and König, 2019). Here, we use the average spectrum ~~(Figure 2)~~. The large standard deviation may be attributed to surface metamorphism during the measurement (Figure 2B).

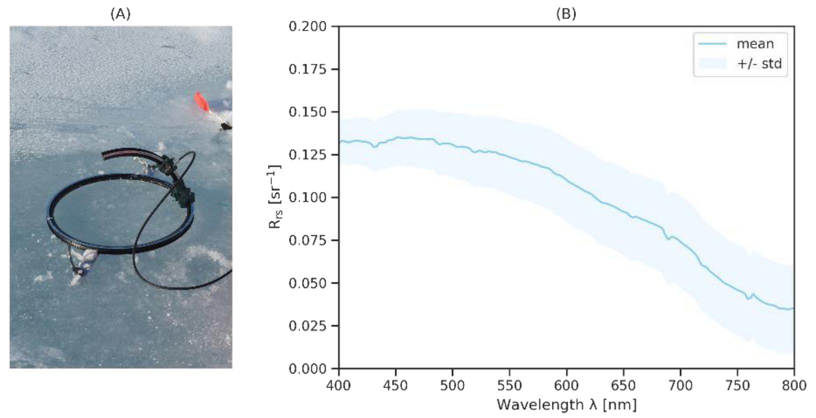

Figure 2: Ibsen bare ice measurement setup (A). Spectra used in this study (B) were taken at nadir.

2.1.2 Pond measurements

On 10 June 2017, we collected 49 melt pond spectra (Gege et al., 2019) and corresponding pond depths in three melt ponds. Two of the ponds had a bright blue color while the third one was very dark, which is also apparent in Figure 3. The pond site was located in a ridged area and ~~single~~ ice thickness measurements from June 31, 2017 showed that ice thickness was ≥ 0.9 m below the bright ponds and ≤ 0.5 m below the dark pond indicating that the bright ice is older. We presume that he dark ice may have been a refrozen lead. However, no ice cores were analyzed to determine the respective ice types.

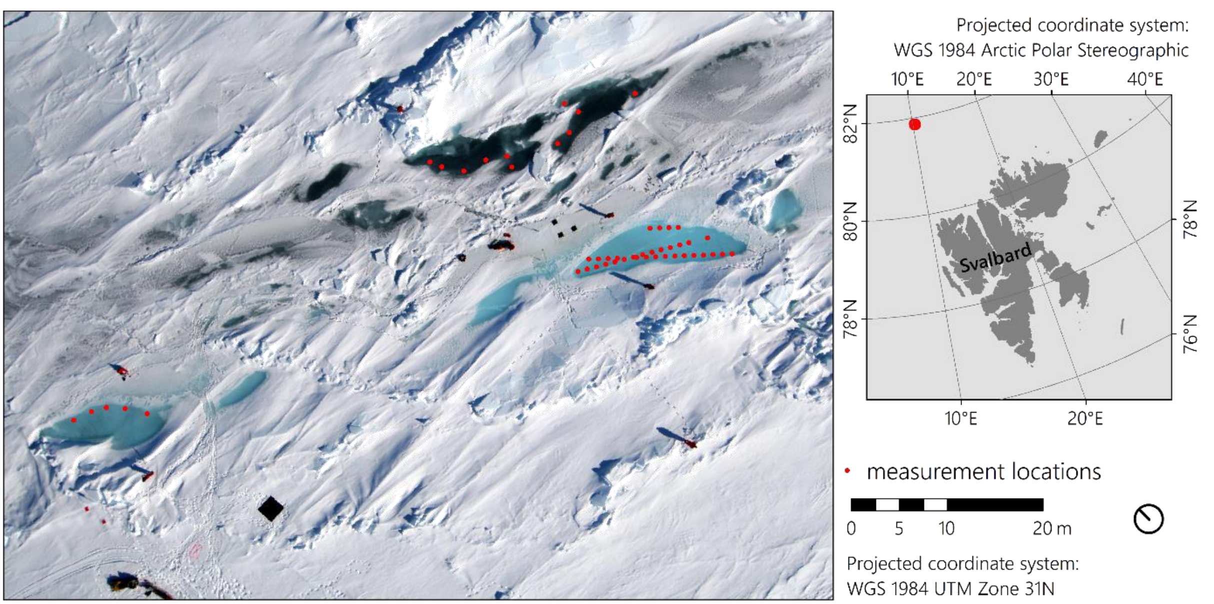

Figure 3: Overview of measurement sites in the three ponds. Aerial photo: Gerit Birnbaum.

Bottoms of the bright ponds were mostly smooth and solid but also featured few cracks and highly scattering areas that were very porous. The dark pond bottom was more heterogeneous and featured cracks and areas that were porous and riddled with holes (Figure 4).

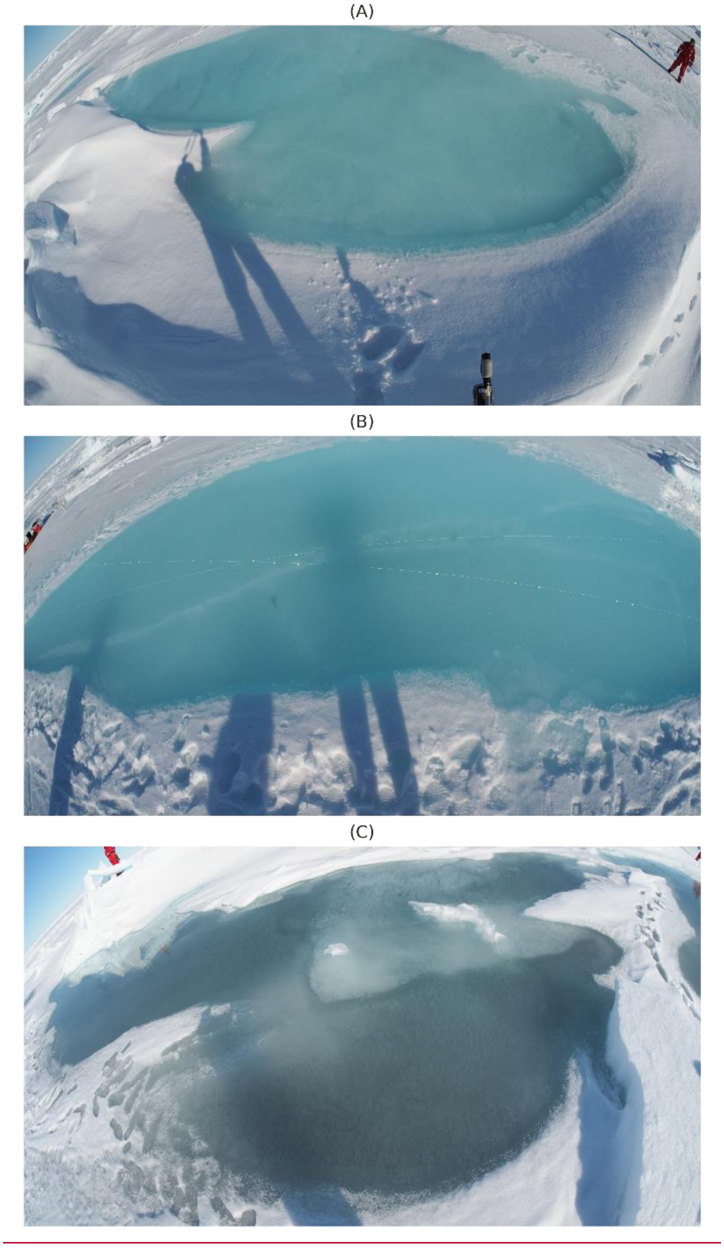

Figure 4: Photos of the small (A) and large (B) bright and the dark pond (c). Photos: Peter Gege.

At each pond, we referenced the Ocean Optics spectrometers using the Spectralon panel before data acquisition. We performed spectral measurements from the edge of the pond or waded through the pond avoiding shading. We did not observe any wind induced disturbances of the water surface and waited for the water surface to settle before performing measurements inside the ponds. All measurements were performed under clear sky conditions between ~~11~~12:~~45~~ 23 ~~UTC~~ local solar time and 14:~~05~~43 ~~UTC~~local solar time, and corresponding sun zenith angles between 58.90° and 61.04°. Directly after each spectral measurement, we used a folding ruler to measure pond depth at the same location. Depths ranged between 6 cm and 25 cm with an average of 17.60 cm. Figure 5~~Figure 4~~ illustrates the melt pond spectra and corresponding pond depths.

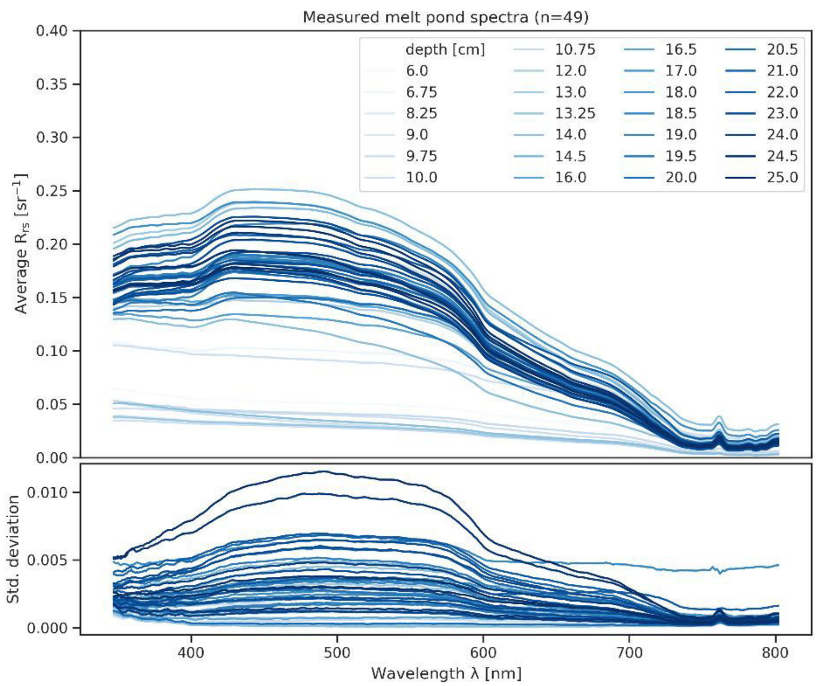

Figure 54: Average reflectance spectra (top), standard deviations of 30 measurements (bottom) and corresponding pond depths.

2.1.3 Data smoothing

Even though the spectra appear smooth at first view, the hardly visible amount of noise in the data becomes relevant for calculating derivatives. To smooth the spectra, we therefore resampled all spectra to a 1 nm spectral sampling by linear interpolation, and then applied a running average filter with a width of 5 nm.

2.2 Model development

To develop an approach that does not require ~~expert~~ knowledge about on site ice characteristics, our model must be independent from changes of the bottom albedo, i.e. scattering characteristics of the underlying ice. It shall further be applicable to a wide range of pond depths up to 1.0 m. Because the in situ melt pond dataset is limited to shallow depths and biased towards bright blueish ponds, we used the Water Color Simulator (WASI) to create a spectral library covering different bottom type mixtures and depths. WASI is a software tool for the analysis and simulation of deep- and shallow-water spectra that bases on well-established analytical models (Gege, 2004, 2014, 2015; Gege and Albert, 2006). We used the forward mode of the program WASI-2D (v4.1) to generate ~~spectral~~ libraries of melt pond spectra. The procedures are described in the following.

2.2.1 Simulated data

We used the Ocean Optics bare ice spectra from overcast sky conditions (Sect. 2.1.1 Ice spectra) as pond bottom reflectance. Analyses of optical properties of water samples showed only negligible amounts of chlorophyll-a, colored dissolved organic matter and total suspended matter. Moreover, Podgorny and Grenfell (1996) report that the signal of scattering in melt water is overwhelmed by the scattering in the bottom ice. We therefore defined a pure water column without absorbing or scattering water constituents and computed remote sensing reflectance in shallow water above the water surface according to Eq. 2.20b in Gege (2015):

$$R_{rs}^{sh}(\lambda) = \frac{(1-\sigma)(1-\sigma_L^-)}{n_W^2} \cdot \frac{R_{rs}^{sh-}(\lambda)}{1-\rho_u \cdot Q \cdot R_{rs}^{sh-}(\lambda)} + R_{rs}^{surf}(\lambda)\ , \qquad (4)$$

where σ, σ_L^- and ρ_u are the reflection factors for E_d and upwelling radiance (L_u^-) and irradiance just below the water surface. σ and ρ_u are 0.03 and 0.54, respectively, while σ_L^- is calculated from the viewing angle (0° for a nadir-directed sensor). n_w is the refractive index of water (≈ 1.33) and Q is a measure of the anisotropy of the light field in water, approximated as 5 sr. R_{rs}^{sh-} is the remote sensing reflectance just below the water surface according to Albert and Mobley (2003):

$$R_{rs}^{sh-}(\lambda) = R_{rs}^{-}(\lambda) \cdot \left[1 - A_{rs,1} \cdot \exp\left\{-\left(K_d(\lambda) + k_{uW}(\lambda)\right) \cdot z_B\right\}\right] + A_{rs,2} \cdot R_{rs}^{b}(\lambda) \cdot \exp\{-K_d(\lambda) + k_{uB}(\lambda)) \cdot z_B\}, \qquad (5)$$

where $A_{rs,1}$ and $A_{rs,2}$ are empirical constants, K_d, k_{uW} and k_{uB} describe the attenuation of the water body with depth z_B defined by its absorption and backscattering, and the viewing and illumination geometry. The first part of Eq. (5) describes the contribution of the water body and the second part the contribution of the bottom. R_{rs}^{-} is the remote sensing reflectance of deep water just below the water surface defined by absorption and backscattering of the water body and the viewing and illumination geometry. R_{rs}^{b} is the remote sensing reflectance of the bottom that is defined as the sum of the fractional radiances of all contributing bottom types defined by their albedos and under the assumption of isotropic reflection. R_{rs}^{surf} in Eq. (4) is the ratio of radiance reflected by the water surface and E_d. We set R_{rs}^{surf} to zero; thus, the last part of Eq. (4) can be ignored. We further used a sun zenith angle of 60°, similar to the in situ measurements, and a viewing angle of 0° (nadir).
We computed linear mixtures of the two measured bottom albedos in 25 % steps (100 % dark, 0 % bright; 75 % dark, 25 % bright; …; 0 % dark, 100 % bright). Using this setup, we generated a spectral look up table (LUT) by increasing pond depth from 0 to 100 cm in intervals of 1 cm, adequate for the great majority of melt ponds on Arctic sea ice. The final LUT contains 505 spectra (Figure 6~~Figure 5~~).

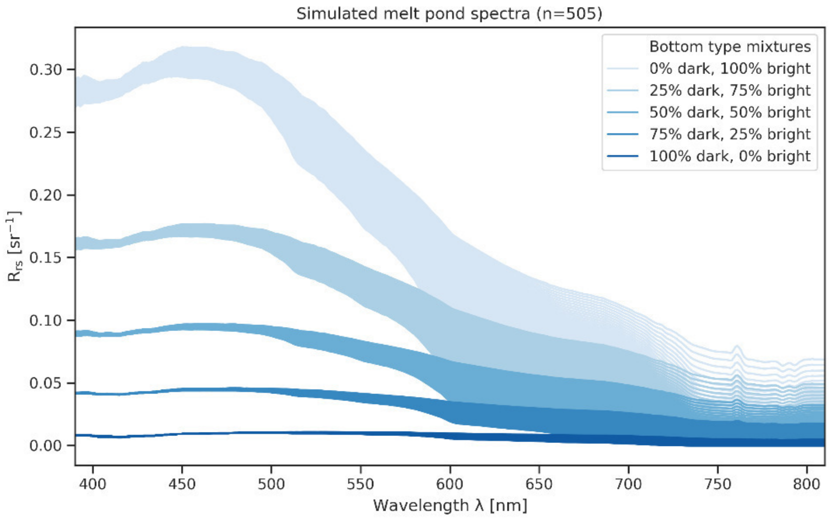

Figure 6~~5~~: LUT generated with WASI-2D. Each of the five bottom type mixtures consists of 101 spectra (0 cm to 100 cm in 1 cm steps).

2.2.2 Data Processing

According to the Beer–Lambert law, the extinction of light at a certain wavelength in a medium is described by an exponential function. Here we assume that multiple scattering in melt water and (multiple) reflections at the pond surface, bottom and sidewalls can be neglected to approximate the radiative transfer. Figure 7~~Figure 6~~A illustrates the exponential decrease of R_{rs} with water depth at 700 nm for the five different bottom type mixtures. To linearize the effect, we computed the logarithm of the spectra (Figure 7~~Figure 6~~B). Lastly, we computed the first derivative of the logarithmized spectra (Figure 7~~Figure 6~~C) for each band by applying a Savitzky-Golay filter using a second order polynomial fit on a 9 nm window (The Scipy community, 2019b).

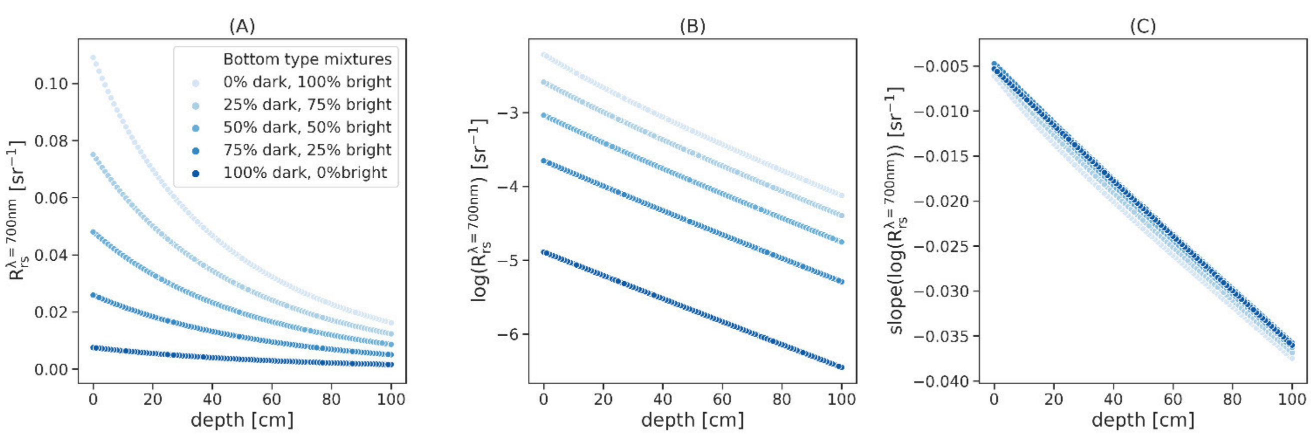

Figure 7~~6~~: Processing of spectral data exemplified for λ = 700 nm.

We then computed Pearson's correlation coefficient (r) as (The Scipy community, 2019c):

$$r(x,y) = \frac{\sum_{i=0}^{n-1}(x_i-\acute{x})(y_i-\acute{y})}{\sqrt{\sum_{i=0}^{n-1}(x_i-\acute{x})^2 \sum_{i=0}^{n-1}(y_i-\acute{y})^2}}, \tag{6}$$

where x_i and $\acute{x}$ are the depth of the i-th sample and the average depth and y_i and $\acute{y}$ are the slope of the logarithmized reflectance at a certain wavelength of the i-th sample and the average slope of the logarithmized reflectance at a certain wavelength; and n is the number of samples.

The orange curve in Figure 8~~Figure 7~~ illustrates the wavelength dependent correlation coefficients of the slope of the logarithmized spectra and pond depths in the LUT. We observe an almost perfect negative correlation in bands between 700 nm and 750 nm. We performed the same processing as for the simulated spectra for the in situ pond spectra. The blue curve in Figure 8 illustrates the wavelength dependent correlation coefficients of measured pond depth and the slope of the logarithmized in situ spectra. We likewise observe strong negative correlations in the wavelength region around 700 nm.

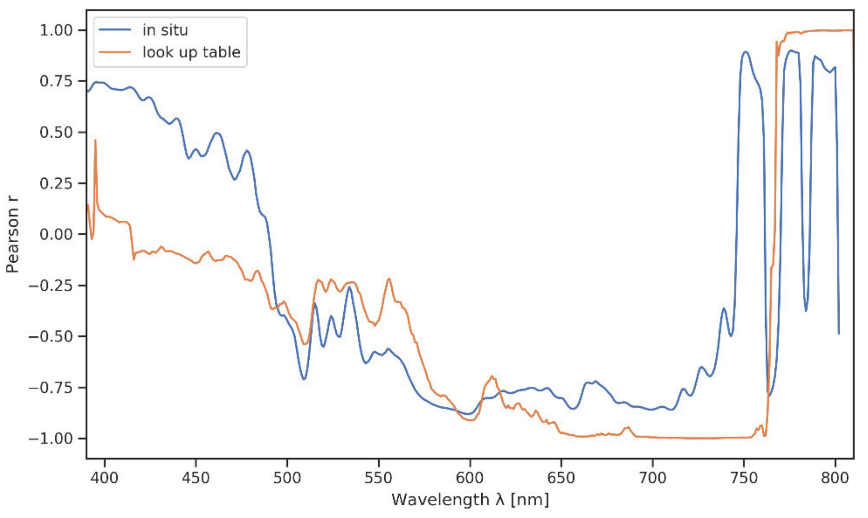

Figure 8~~7~~: Wavelength dependent correlation coefficients of pond depth with slope of log-scaled spectra for in situ measurements and simulated spectra.

To investigate the similarity of the dark and bright ice spectra, we normalized both bottom spectra at 710 nm and found a high spectral similarity between ~ 590 nm and ~ 800 nm (Figure 9~~Figure 8~~). Consequently, the slope of the logarithmized spectra is widely independent from the chosen bottom albedo in this wavelength region. Assuming that this also applies to ice spectra recorded under clear sky conditions, we used the Ibsen bare ice measurement to develop a model for clear sky conditions accordingly.

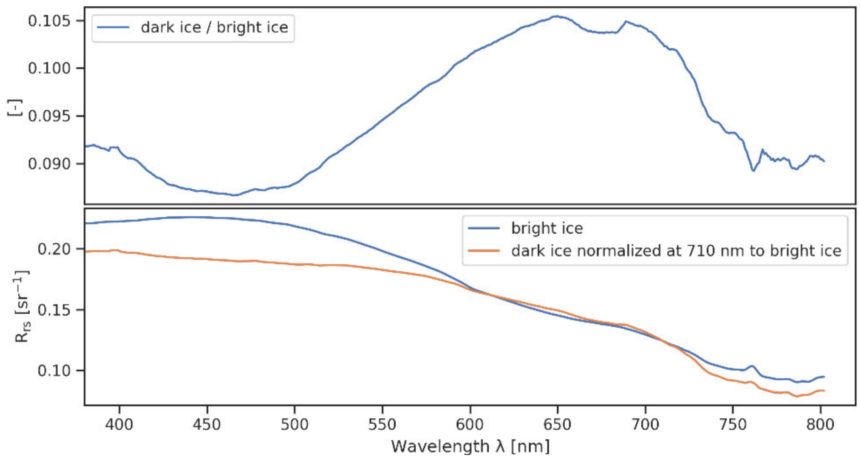

Figure 9~~8~~: Quotient of bright and dark bare ice spectra (top) and R_{rs} of bright ice and dark ice normalized at 710 nm (bottom).

2.2.3 Linear model

Due to the strong negative correlation in the simulated as well as in the measured data, we chose the slope of the logarithmized spectrum at 710 nm (r = -1.0 and -0.86 for simulated and in situ data, respectively) to develop a simple linear model. We used scikit-learn's Linear Regression function (Pedregosa et al., 2011) to fit a linear model to the simulated data with the Ibsen bare ice spectrum as bottom albedo using the method of Ordinary Least Squares.

We found that the solar zenith angle affects the slope and y-intercept of the linear model. Because the model shall be applicable to a wide range of sun zenith angles, we implemented a second model to derive slope and y-intercept of the linear model for various sun zenith angles. We used WASI to generate spectral libraries for different sun zenith angles (0°, 15°, 30°, 45°, 60°, 75°, 90°) and found that the resulting change of slope and y-intercept can each be described by an s-shaped curve. We used SciPy's optimize.curve_fit function (The Scipy community, 2019a) to fit generalized logistic functions (Richards, 1959) into the data. Using these functions, the model's slope and y-intercept can be computed for different sun zenith angles (Figure 10~~Figure 9~~).

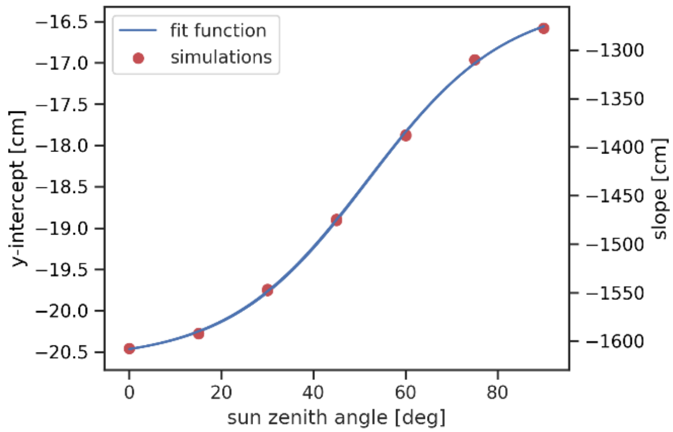

Figure 10~~9~~: Change of model's y-intercept and slope with sun zenith angle. Generalized logistic function fit into the simulated data.

The model is

$$z = a(\theta_{sun}) + b(\theta_{sun}) \left[\frac{\partial log\ R_{rs}(\lambda)}{\partial \lambda}\right]_{\lambda=710\ nm} \tag{7}$$

where z is the predicted pond depth and θ_{sun} is the sun zenith angle. a and b are offset and slope:

$$a(\theta_{sun}) = -20.6 + \frac{0.79}{0.8+5.8\exp(-0.13\cdot\theta_{sun})^{\frac{1}{2}}}\ [cm] \tag{8}$$

and

$$b(\theta_{sun}) = -1619.8 + \frac{94743.64}{255.3+7855\exp(-1.3\cdot\theta_{sun})^{\frac{1}{19.9}}}\ [cm] \tag{9}$$

We further computed the coefficient of determination (R^2) as recommended by Kvålseth (1985) as:

$$R^2(y,\hat{y}) = 1 - \frac{\sum_{i=0}^{n-1}(y_i-\hat{y}_i)^2}{\sum_{i=0}^{n-1}(y_i-\acute{y})^2}, \tag{10}$$

where y_i and $\hat{y}_i$ are the true (simulated) and predicted value of the i-th sample, n is the number of samples and $\acute{y}_i = \frac{1}{n}\sum_{i=0}^{n-1} y_i$ (Pedregosa et al., 2011; scikit-learn developers, 2018). In addition, we also computed the root-mean-square error ($RMSE$) ~~according to Pedregosa et al. (2011) and scikit-learn developers (2018a)~~ as:

$$RMSE(y,\hat{y}) = \sqrt{\frac{1}{n}\sum_{i=0}^{n-1}(y_i - \hat{y}_i)^2}, \tag{11}$$

For the model described above we obtained a perfect correlation (r = 1.0; probability value (p) = 8.9e^{-172}), an R^2 of 1.0 and an $RMSE$ of 0.56 cm on the simulated training data.

3 Results

We validated the model with the in situ melt pond dataset from dark and bright ponds (Sect. 2.1.2 Pond ~~2.1.2 Pond~~) and observed a strong linear and statistically significant correlation (r = 0.86; p = 2.36e^{-15}; R^2 = 0.65 and $RMSE$ = 3.29 cm). Most of the points scatter along the 1:1 line, except for one point where actual depth is 10 cm and predicted depth is 18~~.17~~ cm (Figure 11~~Figure 10~~A). The externally studentized residual (t) (Kutner et al., 2004; Seabold and Perktold, 2010) classifies this point as an outlier (t > 3) and therefore we excluded this point from the data set. The removal of the outlier improves all performance measures (r = 0.89; p = 4.34e^{-17}, R^2 = 0.68, $RMSE$ = 3.11 cm). The slope of the line of best-fit increases to 0.9686 and the intercept indicates an offset of 0.878 cm. If we further correct for the offset R^2 increases to 0.74 and $RMSE$ improves to 2.81 cm. The blue line is the line of best fit between actual and predicted pond depths. The linear equation of the line of best fit indicates that the model results in a small offset and a slope close to 1.0.

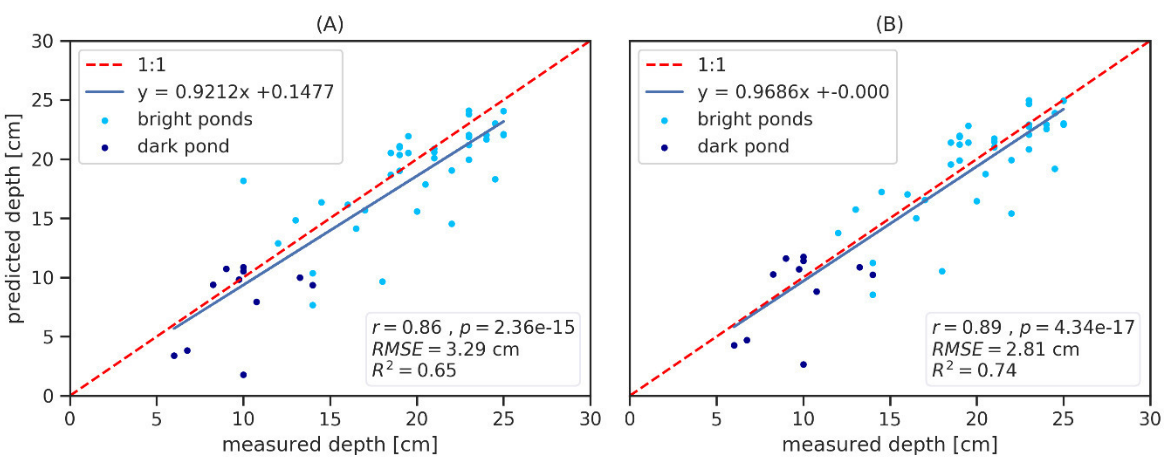

Figure 11~~10~~: Measured vs. predicted depth for the entire dataset (A), with outlier removed and offset correction (B).

4 Discussion

Our results show that a simple model based on the derivative of the log-scaled R_{rs} at 710 nm allows water depth retrieval of dark and bright melt ponds on Arctic sea ice. The model training on simulated data and the independent testing using in situ measurements prove the ~~universality~~ applicability of our approach.

4.1 Observational data

~~To our knowledge, the data used in this study is the most comprehensive set of R_{rs} and depth measurements from Arctic melt ponds acquired under clear sky conditions.~~

4.1.1 Spectral measurements

Measurement of albedo have a long tradition in Arctic research (e.g. Grenfell, 2004; Nicolaus et al., 2010; Perovich, 2002; Perovich and Polashenski, 2012) because ~~albedo~~ it is an important quantity in climate models and can be measured with a single irradiance detector. In this study, we conducted measurements of R_{rs} because our model should be applicable to remote sensing data and ~~it is~~ the ~~most popular~~ quantity measured in optical remote sensing is radiance. Converting albedo to radiance is only possible when assuming a ~~l~~Lambertian scattering behaviour. This assumption, however, is not valid for specular water surfaces and may easily introduce errors. ~~and less sensitive to external environmental conditions while being sensitive to the inherent optical properties of a water body (Mobley et al., 2018).~~ Morassutti and Ledrew (1996) identified changing E_d as the main error affecting reflectance data recording. To tackle this issue, we used a combination of two spectrometers described in Sect. 2.1 Observational data~~2.1 Observational data~~.

Field spectroscopy is influenced by external factors and the measurement design itself. In contrast to ruler measurements, the spectrometer acquires information of an area. To ease comparison and limit the influence of spatial heterogeneities, we used a fore optic with a 1° FOV to minimize the footprint (~ 1 cm at a height of 60 cm). However, holding the instruments perfectly still for a period of several seconds is challenging and even small changes in the position result in changes of the viewing angle, which increase the footprint of a measurement. For future campaigns, we therefore recommend using a gimbal to minimize the influence of roll and pitch of the hand-held spectrometer setup. Another issue might have been reflections of the black spectrometer housings at the water surface possibly contributing~~e~~ to the offset between modeled and measured data. Different refraction indices of wet and dry surfaces may cause part of the observed offset. Furthermore, using bottom albedos obtained from dry surfaces in WASI introduce a systematic offset. However, it remains unclear if the ice surface used to compute the spectral library was wet or dry.

Some of the scattering may be introduced by reflectances at the water surface, which we did not consider in the LUT computation because the necessary values for the parametrization are unknown. Another influence may be the different sun zenith angles between bare ice and pond measurements. The potential influence of the mentioned factors may be worth further examination to refine the model.

4.1.2 Pond depth measurements

Measuring the depth of a pond may appear trivial but the bottom of a pond is frequently not flat and solid but can be slushy or riddled with holes. In addition, performing two measurements with a spectrometer and a folding ruler at the ~~hitting the~~ exact same location is difficult~~spot of the spectral measurement perpendicularly with a folding ruler is tricky~~. We therefore recommend using a laser pointer at the end of the pole for orientation. These uncertainties explain some of the scattering in Figure 11~~Figure 10~~. Interpretation of field photographs of the pond bottoms however did not indicate any systematic errors associated with pond bottom characteristics.

4.2 Model validity

The majority of the field data used in this study ~~is~~ are from bright blue ponds (n=38) while fewer measurements were obtained in dark ponds (n=11). We addressed this limited diversity of field data by computing a comprehensive LUT. The model generates accurate results ($RMSE$ = 2.81 cm) on the entire in situ test data set and explains a large portion of its variability (R^2 = 0.74)~~, but further investigation is necessary to explore its capabilities to derive pond depths > 25 cm.~~. On the ~~sub~~ data set from the dark pond R^2 is < 0. The reason is that measurements from the dark pond are very shallow (6 – 14 cm) and, thus, relative errors are larger compared to the deeper bright ponds. In addition, the number of data points is very small and single outliers have a strong influence on performance metrics. The range of scattering around the 1:1 line (Figure 11) however is similar for the data from dark ($RMSE$ = 3.05 cm) and bright ponds ($RMSE$ = 2.49 cm), proving that the model's accuracy is similar for both subsets.

~~Although t~~The data used in this study are the most comprehensive set of R_{rs} and depth measurements from melt ponds on Arctic sea ice acquired under clear sky conditions. The data set, however,~~, it is~~origins from only three ponds, covering a limited variability of bottom characteristics and pond depth. More ~~data for~~ validation data are desirable to explore the model~~s~~ capabilities to derive pond depth from deep dark and shallow bright ponds, for pond depth > 25 cm and for a wider range of bottom types and sun zenith angles. In addition, more tests are necessary to explore how the model performs when the assumptions formulated in Sect. 2.2 are violated, e.g. when algae, suspended matter or yellow substances are abundant in the pond water or in the ice below the pond.

We successfully developed a model to accurately derive the depth of melt ponds on Arctic sea ice without having to consider ~~that is widely independent from~~ the bottom ice characteristics of the pond; yet, we assume that we cannot entirely avoid any influence. When fitting a model to the Ocean Optics LUT (Figure 7~~Figure 6~~C), we observe scattering around the 1:1 line resulting in $RMSE$ of 1.88 cm. In the Ocean Optics LUT, however, the only variable parameter is bottom type mixture; we therefore conclude that the scattering results from the difference in bottom albedo. Consequently, bottom albedo may affect the model, which may explain some of the scattering in the test data.

Optical satellite data can only be obtained under clear sky conditions but remote sensing images are likewise acquired from helicopters and UAVs. These platforms also operate under diffuse illumination conditions, which are frequent in the Arctic. To check the validity of the model for overcast conditions, we applied the clear sky model to data from the same area acquired on 14 June 2017 during diffuse illumination conditions. The performance, however, is low (Figure 12~~Figure 11~~) and shows a moderate correlation (r = 0.64; p = 2.6e^{-4}), an R^2 < 0 and an $RMSE$ of 12.76 cm. We attribute the low performance to the different illumination conditions. Under diffuse conditions a considerable part of the reflectance measured above the water surface is due to reflection of clouds at the water surface. Further, the optical path length of the incoming light in water changes under overcast conditions.

We therefore conclude that due to the settings of the field measurements, the present model is valid for clear sky conditions with sun zenith angles between 58.9° and 61°. To enlarge its validity range more field data covering different weather and illumination conditions is necessary.

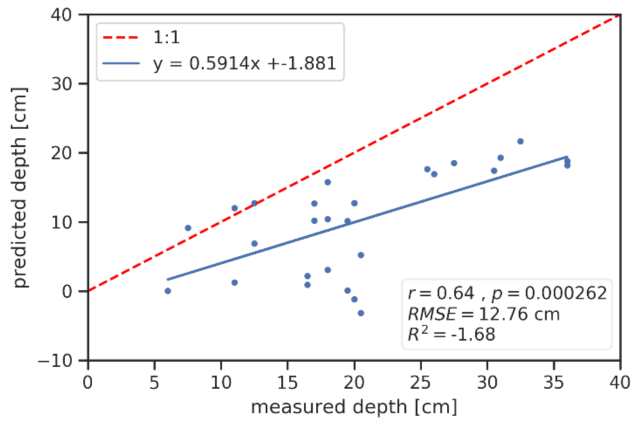

Figure 12~~11~~: Measured vs. predicted water depth for data acquired under overcast conditions on 14 June 2017.

5 Conclusion

We present a linear model slope-based ~~on a slope as a function of depth~~ approach in the spectral region around 710 nm to retrieve the depth of melt ponds on Arctic sea ice. However, the model is not restricted to Arctic sea ice and ~~it~~ may be ~~worth~~ tested~~ing~~ ~~the model's performance~~ in shallow supraglacial ponds as well. The separation of model calibration on simulated data and validation on in situ data proves the ~~universality~~ applicability and robustness of our approach. The final model is valid for hyperspectral data (R_{rs}) acquired under clear sky conditions and addresses varying sun zenith angles. ~~and has been tested on a range of sun zenith angles between 58.9° and 61°.~~

We used WASI to generate a LUT of pond spectra for five different bottom albedos and pond depths between 0 and 100 cm assuming clear pond water. We found that the slope of the log-scaled R_{rs} at 710 nm is widely independent from the bottom albedo and highly correlated with pond depth. Thus, we applied a linear model to retrieve pond depth from R_{rs} in this wavelength region. Slope and y-intercept of the linear equation, however, change with sun zenith angle for which other models do not account for (e.g. Legleiter et al., 2014; Tedesco and Steiner, 2011). To overcome this limitation, we trained linear models for seven sun zenith angles and found that a general logistic function is able to describe the change of slope and y-intercept for each sun zenith angle. The inputs for our model therefore are the slope of the log-scaled $R_{rs}^{\lambda=710}$ and sun zenith angle. We successfully validated the model on in situ measurements ~~from bright and dark ponds~~ ($R^2 = 0.74$, $RMSE = 2.81$ cm) with sun zenith angles between 58.9° and 61° and observed similar accuracies for bright and dark ponds~~and has been tested on a range of sun zenith angles between 58.9° and 61°.~~.

The next step is the transfer to hyperspectral airborne and satellite systems, e.g. EnMAP (Guanter et al., 2016), to enable a synoptic view on the evolution of melt ponds ~~in~~ on Arctic sea ice. One constraint may be the size of melt ponds~~, especially during melt onset and early pond development, which~~, which requires a high spatial resolution. We further assume that the additive signals of the water surface and the atmosphere on the spectrum measured at a ~~satellite~~ remote sensor may complicate the retrieval of pond depth. In addition, the sensitivities and band settings of remote sensors also affect the transferability of our approach. Here, further testing and comprehensive ground truth data ~~is~~ are necessary. In these regards, we expect the Multidisciplinary drifting Observatory for the Study of Arctic Climate (MOSAiC) expedition to result in further improvements.

References

Albert, A. and Mobley, C.: An analytical model for subsurface irradiance and remote sensing reflectance in deep and shallow case-2 waters, Opt. Express, 11(22), 2873, doi:10.1364/OE.11.002873, 2003.

Curry, J. a., Schramm, J. L. and Ebert, E. E.: Sea Ice-Albedo Climate Feedback Mechanism, J. Clim., 8(2), 240–247, doi:10.1175/1520-0442(1995)008<0240:SIACFM>2.0.CO;2, 1995.

Flocco, D., Schroeder, D., Feltham, D. L. and Hunke, E. C.: Impact of melt ponds on Arctic sea ice simulations from 1990 to 2007, J. Geophys. Res. Ocean., 117(C9), n/a-n/a, doi:10.1029/2012JC008195, 2012.

Gege, P.: The water color simulator WASI: an integrating software tool for analysis and simulation of optical in situ spectra, Comput. Geosci., 30(5), 523–532, doi:10.1016/j.cageo.2004.03.005, 2004.

Gege, P.: WASI-2D: A software tool for regionally optimized analysis of imaging spectrometer data from deep and shallow waters, Comput. Geosci., 62, 208–215, doi:10.1016/j.cageo.2013.07.022, 2014.

Gege, P.: The Water Colour Simulator WASI User manual for WASI version 4.1., 2015.

Gege, P. and Albert, A.: A Tool for Inverse Modeling of Spectral Measurements in Deep and Shallow Waters, Situ, 81–109, 2006.

Gege, P. and König, M.: HCRF measurements (Ibsen Freedom VIS FSV-305) of bare Arctic sea ice acquired during POLARSTERN cruise PS106/2, , doi:doi.pangaea.de/10.1594/PANGAEA.908073, 2019.

Gege, P., König, M. and Oppelt, N.: Reflectance measurements (Ocean Optics STS-VIS) of bare ice and melt ponds on Arctic sea ice acquired during POLARSTERN cruise PS106/1, , doi:doi.pangaea.de/10.1594/PANGAEA.908074, 2019.

Grenfell, T. C.: Seasonal and spatial evolution of albedo in a snow-ice-land-ocean environment, J. Geophys. Res., 109(C1), C01001, doi:10.1029/2003JC001866, 2004.

Guanter, L., Kaufmann, H., Foerster, S., Brosinsky, A., Wulf, H., Bochow, M., Boesche, N., Brell, M., Buddenbaum, H., Chabrillat, S., Hank, T., Heiden, U., Heim, B., Heldens, W., Hill, J., Hollstein, A., Hostert, P., Krasemann, H., Leitão, P. J., van der Linden, S., Mauser, W., Mielke, C., Müller, A., Oppelt, N., Roessner, S., Röttgers, R., Schneiderhan, T., Staenz, K. and Segl, K.: EnMAP Science Plan. EnMAP Technical Report., 2016.

Holland, M. M., Bailey, D. A., Briegleb, B. P., Light, B. and Hunke, E.: Improved sea ice shortwave radiation physics in CCSM4: The impact of melt ponds and aerosols on Arctic sea ice, J. Clim., 25(5), 1413–1430, doi:10.1175/JCLI-D-11-00078.1, 2012.

Hunke, E. C., Hebert, D. A. and Lecomte, O.: Level-ice melt ponds in the Los Alamos sea ice model, CICE, Ocean Model., 71, 26–42, doi:10.1016/j.ocemod.2012.11.008, 2013.

Ibsen Photonics: FREEDOM VIS Product Sheet, [online] Available from: https://ibsen.com/wp-content/uploads/Ibsen-Product-Sheets-FREEDOM-VIS.pdf, 2019.

Inoue, J., Kikuchi, T. and Perovich, D. K.: Effect of heat transmission through melt ponds and ice on melting during summer in the Arctic Ocean, J. Geophys. Res. Ocean., 113(5), 1–13, doi:10.1029/2007JC004182, 2008.

Istomina, L., Heygster, G., Huntemann, M., Schwarz, P., Birnbaum, G., Scharien, R., Polashenski, C., Perovich, D., Zege, E., Malinka, A., Prikhach, A. and Katsev, I.: Melt pond fraction and spectral sea ice albedo retrieval from MERIS data - Part 1: Validation against in situ, aerial, and ship cruise data, Cryosphere, 9(4), 1551–1566, doi:10.5194/tc-9-1551-2015, 2015a.

Istomina, L., Heygster, G., Huntemann, M., Marks, H., Melsheimer, C., Zege, E., Malinka, A., Prikhach, A. and Katsev, I.: Melt pond fraction and spectral sea ice albedo retrieval from MERIS data - Part 2: Case studies and trends of sea ice albedo and melt ponds in the Arctic for years 2002-2011, Cryosphere, 9(4), 1567–1578, doi:10.5194/tc-9-1567-2015, 2015b.

Istomina, L., Melsheimer, C., Huntemann, M. and Nicolaus, M.: Retrieval of Sea Ice Thickness During Melt Season From in Situ , Airborne and Satellite Imagery, , 7678–7681, 2016.

Kutner, M. H., Li, W., Nachtsheim, C. J. and Neter, J.: Applied Linear Statistical Models, Fifth edit., 2004.

Kvålseth, T. O.: Cautionary Note about R 2, Am. Stat., 39(4), 279–285, doi:10.1080/00031305.1985.10479448, 1985.

Lecomte, O., Fichefet, T., Vancoppenolle, M. and Nicolaus, M.: A new snow thermodynamic scheme for large-scale sea-ice models, Ann. Glaciol., 52(57), 337–346, doi:10.3189/172756411795931453, 2011.

Lee, S. H., Stockwell, D. A., Joo, H.-M., Son, Y. B., Kang, C.-K. and Whitledge, T. E.: Phytoplankton production from melting ponds on Arctic sea ice, J. Geophys. Res. Ocean., 117(C4), n/a-n/a, doi:10.1029/2011JC007717, 2012.

Legleiter, C. J., Tedesco, M., Smith, L. C., Behar, A. E. and Overstreet, B. T.: Mapping the bathymetry of supraglacial lakes and streams on the Greenland ice sheet using field measurements and high-resolution satellite images, Cryosph., 8(1), 215–228, doi:10.5194/tc-8-215-2014, 2014.

Liu, J., Song, M., Horton, R. M. and Hu, Y.: Revisiting the potential of melt pond fraction as a predictor for the seasonal Arctic sea ice extent minimum, Environ. Res. Lett., 10(5), 054017, doi:10.1088/1748-9326/10/5/054017, 2015.

Lu, P., Leppäranta, M., Cheng, B. and Li, Z.: Influence of melt-pond depth and ice thickness on Arctic sea-ice albedo and light transmittance, Cold Reg. Sci. Technol., 124, 1–10, doi:10.1016/j.coldregions.2015.12.010, 2016.

Lu, P., Leppä, M., Cheng, B., Li, Z., Istomina, L. and Heygster, G.: The color of melt ponds on Arctic sea ice, , 8(August), 1–24, 2017.

Malinka, A., Zege, E., Istomina, L., Heygster, G., Spreen, G., Perovich, D. and Polashenski, C.: Reflective properties of melt ponds on sea ice, Cryosph., 12(6), 1921–1937, doi:10.5194/tc-12-1921-2018, 2018.

Morassutti, M. P. and Ledrew, E. F.: Albedo and depth of melt ponds on sea-ice, Int. J. Climatol., 16(7), 817–838, 1996.

Nicolaus, M., Gerland, S., Hudson, S. R., Hanson, S., Haapala, J. and Perovich, D. K.: Seasonality of spectral albedo and transmittance as observed in the Arctic Transpolar Drift in 2007, J. Geophys. Res. Ocean., 115(11), 1–21, doi:10.1029/2009JC006074, 2010.

Ocean Optics: STS-VIS SPECS, [online] Available from: https://oceanoptics.com/product/sts-vis-microspectrometer/#tab-specifications (Accessed 26 March 2019), 2019.

Palmer, M. A., Saenz, B. T. and Arrigo, K. R.: Impacts of sea ice retreat, thinning, and melt-pond proliferation on the summer phytoplankton bloom in the Chukchi Sea, Arctic Ocean, Deep Sea Res. Part II Top. Stud. Oceanogr., 105, 85–104, doi:10.1016/j.dsr2.2014.03.016, 2014.

Pedersen, C. A., Roeckner, E., Lüthje, M. and Winther, J.: A new sea ice albedo scheme including melt ponds for ECHAM5 general circulation model, J. Geophys. Res., 114(D8), D08101, doi:10.1029/2008JD010440, 2009.

Pedregosa, F., Varoquaux, G., Gramfort, A., Michel, V., Thirion, B., Grisel, O., Blondel, M., Prettenhofer, P., Weiss, R., Dubourg, V., Vanderplas, J., Passos, A., Cournapeau, D., Brucher, M., Perrot, M. and Duchesnay, E.: Scikit-learn: Machine Learning in {P}ython, J. Mach. Learn. Res., 12, 2825–2830, 2011.

Perovich, D. K.: Seasonal evolution of the albedo of multiyear Arctic sea ice, J. Geophys. Res., 107(C10), 1–13, doi:10.1029/2000JC000438, 2002.

Perovich, D. K. and Polashenski, C.: Albedo evolution of seasonal Arctic sea ice, Geophys. Res. Lett., 39(8), 1–6, doi:10.1029/2012GL051432, 2012.

Perovich, D. K., Grenfell, T. C., Light, B., Elder, B. C., Harbeck, J., Polashenski, C., Tucker, W. B. and Stelmach, C.: Transpolar observations of the morphological properties of Arctic sea ice, J. Geophys. Res. Ocean., 114(1), doi:10.1029/2008JC004892, 2009.

Philpot, W. D.: Bathymetric mapping with passive multispectral imagery, Appl. Opt., 28(8), 1569, doi:10.1364/ao.28.001569, 1989.

Podgorny, I. A. and Grenfell, T. C.: Partitioning of solar energy in melt ponds from measurements of pond albedo and depth, J. Geophys. Res. Ocean., 101(C10), 22737–22748, doi:10.1029/96JC02123, 1996.

Polashenski, C., Perovich, D. and Courville, Z.: The mechanisms of sea ice melt pond formation and evolution, J. Geophys. Res. Ocean., 117(C1), 1–23, doi:10.1029/2011JC007231, 2012.

Pope, R. M. and Fry, E. S.: Absorption spectrum (380–700 nm) of pure water II Integrating cavity measurements, Appl. Opt., 36(33), 8710, doi:10.1364/AO.36.008710, 1997.

Richards, F. J.: A Flexible Growth Function for Empirical Use, J. Exp. Bot., 10(2), 290–301, doi:10.1093/jxb/10.2.290, 1959.

Rösel, A., Kaleschke, L. and Birnbaum, G.: Melt ponds on Arctic sea ice determined from MODIS satellite data using an artificial neural network, Cryosph., 6(2), 431–446, doi:10.5194/tc-6-431-2012, 2012.

Schröder, D., Feltham, D. L., Flocco, D. and Tsamados, M.: September Arctic sea-ice minimum predicted by spring melt-pond fraction, Nat. Clim. Chang., 4(5), 353–357, doi:10.1038/nclimate2203, 2014.

scikit-learn developers: R^2 score, the coefficient of determination, [online] Available from: https://scikit-learn.org/stable/modules/model_evaluation.html#r2-score (Accessed 13 February 2019), 2018.

Seabold, S. and Perktold, J.: Statsmodels: Econometric and statistical modeling with python, in 9th Python in Science Conference., 2010.

Tedesco, M. and Steiner, N.: In-situ multispectral and bathymetric measurements over a supraglacial lake in western Greenland using a remotely controlled watercraft, Cryosphere, doi:10.5194/tc-5-445-2011, 2011.

The Scipy community: scipy.optimize.curve_fit, SciPy v1.2.1 Ref. Guid. [online] Available from: https://docs.scipy.org/doc/scipy/reference/generated/scipy.optimize.curve_fit.html (Accessed 11 July 2019a), 2019.

The Scipy community: scipy.signal.savgol_filter, SciPy v1.2.1 Ref. Guid. [online] Available from:

https://docs.scipy.org/doc/scipy/reference/generated/scipy.signal.savgol_filter.html?highlight=savgol#scipy.signal.savgol_filter, 2019b.

The Scipy community: scipy.stats.pearsonr, SciPy v1.2.1 Ref. Guid. [online] Available from: https://docs.scipy.org/doc/scipy/reference/generated/scipy.stats.pearsonr.html (Accessed 13 February 2019c), 2019.

Tschudi, M. A., Maslanik, J. A. and Perovich, D. K.: Derivation of melt pond coverage on Arctic sea ice using MODIS observations, Remote Sens. Environ., 112(5), 2605–2614, doi:10.1016/j.rse.2007.12.009, 2008.

Webster, M. A., Rigor, I. G., Perovich, D. K., Richter-Menge, J. A., Polashenski, C. M. and Light, B.: Seasonal evolution of melt ponds on Arctic sea ice, J. Geophys. Res. Ocean., 120(9), 5968–5982, doi:10.1002/2015JC011030, 2015.

Zege, E., Malinka, A., Katsev, I., Prikhach, A., Heygster, G., Istomina, L., Birnbaum, G. and Schwarz, P.: Algorithm to retrieve the melt pond fraction and the spectral albedo of Arctic summer ice from satellite optical data, Remote Sens. Environ., 163, 153–164, doi:10.1016/j.rse.2015.03.012, 2015.

Data availability

The data used in this study are available at the PANGAEA data repository under doi.pangaea.de/10.1594/PANGAEA.908075.

Author contribution

MK and NO conceptualized the study. MK designed the methodology, curated and analysed the data, created and validated the models, visualized results and wrote the original draft. NO critically reviewed the draft and both authors contributed in editing and finalizing the paper.

Competing interests

The authors declare that they have no conflict of interest.

Acknowledgements

We thank Peter Gege for his encouragement and the provision of WASI. We highly appreciate the support by the German Aerospace Center (DLR) Oberpfaffenhofen and especially thank Thomas Schwarzmaier, Stefan Plattner and Peter Gege for the development and provision of the instruments used in this study. We further acknowledge the support of captain Wunderlich, the crew and the chief scientists Andreas Macke and Hauke Flores of RV Polarstern cruise AWI_PS106_00 and value the assistance provided by the colleagues supporting our fieldwork on PS106 especially Peter Gege, Gerit Birnbaum, Niels Fuchs, Martin Hieronymi and Thomas Ruhtz. We would also like to thank Justin Mullins at Write About Science for his valuable comments and Marcel Nicolaus for his estimation of the pond site's ice type situation. Finally, we thank two anonymous referees for their constructive critique, which helped us to improve the manuscript and Stef Lhermitte for his editorial efforts.